

SubZeroCore: A Submodular Approach with Zero Training for Coreset Selection

Brian B. Moser^{1,2}, Tobias C. Nauen^{1,2}, Arundhati S. Shanbhag^{1,2}, Federico Raue¹, Stanislav Frolov¹, Joachim Folz¹, and Andreas Dengel^{1,2}

¹ German Research Center for Artificial Intelligence (DFKI), Germany

² RPTU Kaiserslautern-Landau, Germany

³ Equal Contribution

`first.second@dfki.de`

Abstract. The goal of coreset selection is to identify representative subsets of datasets for efficient model training. Yet, existing approaches paradoxically require expensive training-based signals, e.g., gradients, decision boundary estimates or forgetting counts, computed over the entire dataset prior to pruning, which undermines their very purpose by requiring training on samples they aim to avoid. We introduce SubZeroCore, a novel, training-free coreset selection method that integrates submodular coverage and density into a single, unified objective. To achieve this, we introduce a sampling strategy based on a closed-form solution to optimally balance these objectives, guided by a single hyperparameter that explicitly controls the desired coverage for local density measures. Despite no training, extensive evaluations show that SubZeroCore matches training-based baselines and significantly outperforms them at high pruning rates, while dramatically reducing computational overhead. SubZeroCore also demonstrates superior robustness to label noise, highlighting its practical effectiveness and scalability for real-world scenarios.

1 Introduction

Deep learning breakthroughs often stem from training ever-larger models on ever-larger datasets, a trend that is both resource-heavy and environmentally costly [13, 27, 66, 77]. In many applications, however, collecting or storing vast amounts of data poses significant challenges [19, 72]. Coreset selection seeks to address these problems by identifying a subset that contains a sufficient yet representative data summary of the original dataset [20, 47, 61]. In principle, such a coreset, once found, allows one to train models more efficiently on a fraction of the data without sacrificing much training quality [8, 27]. Sometimes, they even lead to better training performance by mitigating the risk of injecting poisoned data into training, i.e., data with noisy annotations or outliers [6, 27, 41, 56]. Examples of such positive effects can be found in various deep learning fields like neural architecture search [44, 48, 73], image enhancement [15, 35, 45], dataset distillation [11, 28, 46], imbalanced datasets [39, 59], continual learning [9, 51, 74], and even quantum machine learning [22, 55, 71].

An ideal coreset selection method must balance two competing goals: **coverage**, which measures how well a selected subset represents the overall diversity and distribution of the full dataset, and **density**, which identifies highly concentrated regions in the data space containing informative, but potentially redundant samples [32, 57, 77]. Despite recent progress, state-of-the-art methods often incur heavy computational overhead because they rely on training-based signals such as gradients [29, 42, 53], forgetting scores [53, 65], or decision boundary estimates [17, 40]. While these signals can help to identify impactful samples, they require partial or complete model training and are also subject to exhaustive hyperparameter search [20]. Paradoxically, this means current coreset selection methods, intended to reduce training burdens, often require extensive training and evaluations themselves.

In this work, we propose **SubZeroCore**, a novel coreset selection method grounded in submodular optimization [7] that requires *zero model training*. Unlike existing gradient-based or loss-dynamic methods, SubZeroCore uniquely integrates both coverage and density into a single, submodular objective. As such, SubZeroCore positions itself among geometry-based methods like k-center greedy but with an objective for optimizing density as well as coverage. By leveraging a closed-form coverage estimate to compute a hyperparameter-efficient local density, our method systematically picks a suitable neighborhood size with no reliance on gradients or iterative training. The result is a coreset selection method that (i) avoids expensive model-specific signals, (ii) maintains high coverage but still focuses on dense regions, (iii) offers theoretical optimality guarantees through submodularity, and (iv) relies on a single, controllable hyperparameter.

Concretely, we demonstrate that our submodular objective captures both coverage and density to improve the quality of coreset. Our experiments on CIFAR-10 [34] as well as ImageNet-1K [14] show that SubZeroCore consistently performs comparable to training-based baselines for low pruning rates and outperforms them under high pruning rates, while being substantially faster than most training-based approaches. Moreover, as emphasizing dense regions naturally de-emphasizes outliers, SubZeroCore remains robust to label noise.

Taken together, our findings frame SubZeroCore as a practical tool for scalable coreset selection. We believe this approach offers a practical avenue for advancing coreset-based strategies in domains where data curation or resource constraints predominate [1, 36].

2 Preliminaries

2.1 Coreset Selection

We begin with a classical discriminative task, where the training dataset $\mathcal{T} = \{(\mathbf{x}_i, y_i)\}_{i=1}^N$ consists of N i.i.d. samples drawn from an underlying data distribution P . Each input $\mathbf{x}_i \in \mathcal{X}$ is paired with a ground-truth label $y_i \in \mathcal{Y}$.

Definition 1 (Coreset Selection). *The goal of coreset selection is to derive a small subset $\mathcal{S} \subset \mathcal{T}$ ($|\mathcal{S}| \ll |\mathcal{T}|$) such that training a model $\theta^{\mathcal{S}}$ on \mathcal{S} yields generalization performance on par with $\theta^{\mathcal{T}}$ trained on the entire dataset \mathcal{T} :*

$$\mathcal{S}^* = \arg \min_{\mathcal{S} \subset \mathcal{T}: \frac{|\mathcal{S}|}{|\mathcal{T}|} \approx 1-\alpha} \mathbb{E}_{\mathbf{x}, y \sim P} [\mathcal{L}(\mathbf{x}, y; \theta^{\mathcal{S}}) - \mathcal{L}(\mathbf{x}, y; \theta^{\mathcal{T}})], \quad (1)$$

where $\alpha \in (0, 1)$ is the pruning ratio (fraction of samples removed) and \mathcal{L} is a loss function.

While this objective is conceptually straightforward, it can be difficult to realize in practice [2, 4, 18]. One must decide how best to measure “importance” or “representativeness” for each sample \mathbf{x}_i , so that the selection algorithm can prioritize those samples that most benefit the training [52, 60, 63, 70]. For the remainder of this work, we focus on class-wise selection algorithms. Accordingly, we adopt the simplified notation $\mathbf{x} \sim P$ instead of $(\mathbf{x}, y) \sim P$. Thus, we also denote datasets using the simplified notation $\mathcal{T} = \{\mathbf{x}_i\}_{i=1}^N$ and selected coresets as $\mathcal{S} = \{\mathbf{x}_i\}_{i=1}^{(1-\alpha) \cdot N}$.

2.2 Submodular Functions

Submodularity is a fundamental property of set functions that captures the principle of diminishing returns. Since we are interested in selecting the most informative samples first, the submodularity property is especially attractive for coreset selection [16, 25, 26, 33, 67].

Definition 2 (Submodularity). *A function $f : 2^V \rightarrow \mathbb{R}$ defined over a ground set V is called submodular if, for any subsets $A \subseteq B \subseteq V$ and any element $j \in V \setminus B$, it holds that*

$$f(A \cup \{j\}) - f(A) \geq f(B \cup \{j\}) - f(B). \quad (2)$$

This diminishing-returns condition intuitively says that adding an element to a smaller set provides a larger marginal gain than adding it to a bigger set [24].

Formally, coreset selection can be posed as maximizing a submodular function under a budget constraint:

$$\mathcal{S}^* = \arg \max_{\mathcal{S} \subset \mathcal{T}: \frac{|\mathcal{S}|}{|\mathcal{T}|} \approx 1-\alpha} f(\mathcal{S}), \quad (3)$$

where f is submodular, \mathcal{T} indexes all data samples, and α is the pruning factor. A common submodular example is facility location.

Definition 3 (Facility Location). *Facility location [7, 68] defines a submodular function $f_{FL} : 2^{\mathcal{T}} \rightarrow \mathbb{R}$:*

$$f_{FL}(\mathcal{S}) = \sum_{\mathbf{x} \in \mathcal{T}} \max_{\mathbf{x}_S \in \mathcal{S}} \text{sim}(\mathbf{x}, \mathbf{x}_S), \quad (4)$$

where sim is typically a similarity function (e.g., cosine) [25]. The facility location function inherently favors coverage because it evaluates each data sample in the entire dataset by taking the maximum similarity to any sample in the selected subset.

Although finding the exact optimal subset \mathcal{S}^* under a submodular objective f is generally NP-hard [23, 62], submodular functions enjoy a crucial advantage: they can be approximately maximized via a simple greedy algorithm. For the cardinality-constrained case (i.e., limited subset size), the classical result by Nemhauser et al. [50] guarantees that greedy selection achieves a $(1 - 1/e) \approx 63\%$ approximation ratio: $f(\mathcal{S}_{\text{greedy}}) \geq (1 - 1/e) f(\mathcal{S}^*)$. This tells us that (i) greedy selection obtains a strong approximation without exhaustive search, (ii) the greedy algorithm guarantees to achieve at least about 63% of the maximum possible score of the chosen submodular function (such as facility location), and (iii) lazy-greedy optimizations [37, 38] can reduce computational cost significantly. While one might ask “Why not 100%?”, the answer is that each greedy step picks the locally best option at that moment, without accounting for future interactions among samples. Yet, *greedy suboptimality* has been a well-understood limitation in submodular maximization since 1978, but in practice, the $(1 - 1/e)$ bound on the submodular metric score is often considered both strong and acceptable [7, 37, 50].

3 Methodology

The goal of coreset selection is to select data samples that (i) collectively achieve sufficient coverage of the underlying data distribution and (ii) lie in high-density regions. Since both objectives usually counteract each other, existing methods generally choose just one objective: However, for high pruning ratios, one desires a high-density driven coreset selection method, while a coverage-based method is more favorable for low pruning ratios [57, 77].

Thus, balancing both density and coverage within a unified framework remains a significant yet challenging objective. We propose SubZeroCore, a new method that combines submodular optimization, i.e., facility location-based coverage maximization, with density-driven importance weighting, as illustrated in Figure 1.

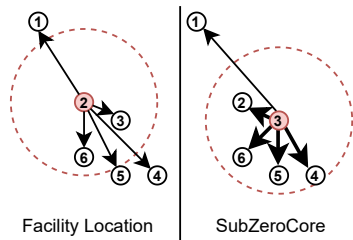


Fig. 1: The goal of SubZeroCore: In addition to maximizing coverage through facility location (**left**), SubZeroCore (**right**) also incorporates a density-based weighting scheme, which prioritizes selecting data samples (red dots) from regions of higher local density as emphasized by the bold arrows.

3.1 Concerning Density

Definition 4 (Density). For a data sample \mathbf{x} , we define its density by finding the size of the neighborhood needed to capture K nearest neighbors in \mathcal{T} . If we

define the radius by $r = \text{NND}_K(\mathbf{x})$, where $\text{NND}_K(\mathbf{x})$ denotes the distance of \mathbf{x} to its K -th nearest-neighbor, then a common way to express density $\rho_K : \mathcal{T} \rightarrow [0, \infty]$ is via

$$\rho_K(\mathbf{x}) = \frac{|B(\mathbf{x}, r) \cap \mathcal{T}|}{\text{Vol}(B(\mathbf{x}, r))}, \quad (5)$$

where $B(\mathbf{x}, r)$ is a ball around \mathbf{x} with radius r , Vol is the volume [43], and $|B(\mathbf{x}, r) \cap \mathcal{T}|$ are the amount of elements in \mathcal{T} within that ball. Note that $|B(\mathbf{x}, r) \cap \mathcal{T}| > K$ can occur when there are multiple neighbors with exactly $\text{NND}_K(\mathbf{x})$ distance to \mathbf{x} (also exemplified later in Figure 2).

Informally, density measures how crowded or populated the local region is, thus high for samples with strong support in the real dataset. For further simplifications, we introduce the following lemma:

Lemma 1. *For a given K and any two samples $\mathbf{x}_i, \mathbf{x}_j \in \mathcal{T}$ it holds that $\text{NND}_K(\mathbf{x}_i) < \text{NND}_K(\mathbf{x}_j) \Leftrightarrow \rho_K(\mathbf{x}_i) > \rho_K(\mathbf{x}_j)$. In other words, a sample that requires a smaller radius to capture K neighbors is in a denser region.*

Proof. Consider $r_{\mathbf{x}_i} = \text{NND}_K(\mathbf{x}_i)$ and $r_{\mathbf{x}_j} = \text{NND}_K(\mathbf{x}_j)$ such that $r_{\mathbf{x}_i} < r_{\mathbf{x}_j}$. Since the volume [43] of a ball in a d -dimensional metric space

$$\text{Vol}(B(\mathbf{x}, r)) = \frac{\pi^{\frac{d}{2}}}{\Gamma(\frac{d}{2} + 1)} r^d$$

is strictly increasing with respect to its radius, it trivially follows that

$$\text{Vol}(B(\mathbf{x}_i, r_{\mathbf{x}_i})) < \text{Vol}(B(\mathbf{x}_j, r_{\mathbf{x}_j})) \Leftrightarrow \rho_K(\mathbf{x}_i) > \rho_K(\mathbf{x}_j).$$

Consequently, the ordering of density for each individual sample \mathbf{x}_i depends by how large or small its ball radius $\text{NND}_K(\mathbf{x}_i) = r_i$ is compared to other samples : (1) If the radius r_i is small, the sample \mathbf{x}_i lies in a densely populated region because its closest neighbors are spatially closer to it. (2) If the radius r_i is large, the sample \mathbf{x}_i lies in a sparsely populated region, implying fewer samples within close proximity.

3.2 SubZeroCore

By integrating the density measure for a single sample as a weighting to the facility location, which maximizes coverage, we straightforwardly derive a submodular function dubbed **SubZeroCore** that encourages both aspects, namely coverage and density.

Definition 5 (SubZeroCore). *Given a data sample $\mathbf{x} \in \mathcal{T}$, we define its density based on Equation 5 by comparing its radius to the overall distribution of neighborhood radii. Simply put, a smaller radius implies higher density (see Lemma Lemma 1). More formally, let $\{r_i\}_{i=1}^{|\mathcal{T}|}$ be the radii derived from a fixed*

K via $r_i = \text{NND}_K(\mathbf{x}_i)$. We compute a sample density score by its relation to the empirical mean $\mu = \frac{1}{|\mathcal{T}|} \sum_{i=1}^{|\mathcal{T}|} r_i$ and standard deviation σ of the radii distribution. We then define a density score

$$s_i = \exp\left(-\frac{(r_i - \mu)^2}{2\sigma^2}\right). \quad (6)$$

By using this normalization, we ensure that density scores are smoothly and consistently assigned, with the highest scores centered around samples whose radii are close to the average density μ , clearly highlighting average dense regions and systematically down-weighting sparse outliers or overly dense inliers. We then feed these density scores into a weighted facility location function $f_{\text{SubZeroCore}} : 2^{\mathcal{T}} \rightarrow \mathbb{R}$:

$$f_{\text{SubZeroCore}}(\mathcal{S}) = \sum_{\mathbf{x}_i \in \mathcal{T}} \max_{\mathbf{x}_j \in \mathcal{S}} (s_j \cdot \text{sim}(\mathbf{x}_i, \mathbf{x}_j)), \quad (7)$$

where \mathcal{T} indexes the entire set of samples in a class, $\mathcal{S} \subseteq \mathcal{T}$ denotes a candidate coreset, and $\text{sim}(\mathbf{x}_i, \mathbf{x}_j)$ is, for instance, a cosine similarity defined on the embeddings of \mathbf{x}_i and \mathbf{x}_j . The term s_j acts as a density-based weight emphasizing samples in averagely crowded regions.

Corollary 1. *The SubZeroCore function $f_{\text{SubZeroCore}}$ is submodular.*

Proof. This directly follows from *Berczi et al.* [7] and can be found in the appendix.

3.3 Impact of the Radius and its Coverage

Radius. The notion of density in dataset pruning heavily relies on the selection of K , which sets the scale at which we measure local density, as shown in Figure 2. This is due to the fact that the volume is monotonically increasing with increasing K and from $B(\mathbf{x}, \text{NND}_K(\mathbf{x})) \subseteq B(\mathbf{x}, \text{NND}_{K+1}(\mathbf{x}))$. Consequently, if K is small, density estimates become overly sensitive to isolated samples (overfitting outliers). Conversely, too large K smooths density differences.

Unfortunately, a balanced selection of K depends on the size of the underlying dataset \mathcal{T} and the pruning ratio α . To address this, we directly tie K to an interpretable, desired coverage target γ between 0% and 100% for the density calculation, thereby systematically guiding the scale at which our method optimally balances coverage with density.

Coverage. Inspired by the image synthesis domain and *Naeem et al.* [49], we define:

Definition 6 (Coverage). *Coverage is a measure for what fraction of \mathcal{T} -neighborhoods contain a sample of the coreset \mathcal{S} . More formally,*

$$\text{coverage}_K(\mathcal{S}, \mathcal{T}) := \frac{1}{|\mathcal{T}|} \sum_{\mathbf{x} \in \mathcal{T}} \mathbf{1}_{\exists \mathbf{x}_S \in \mathcal{S} \text{ s.t. } \mathbf{x}_S \in B(\mathbf{x}, \text{NND}_K(\mathbf{x}))}. \quad (8)$$

where $B(\mathbf{x}, \text{NND}_K(\mathbf{x}))$ is again a ball around \mathbf{x} with radius $\text{NND}_K(\mathbf{x})$, which is defined by its distance to its K -th nearest-neighbor.

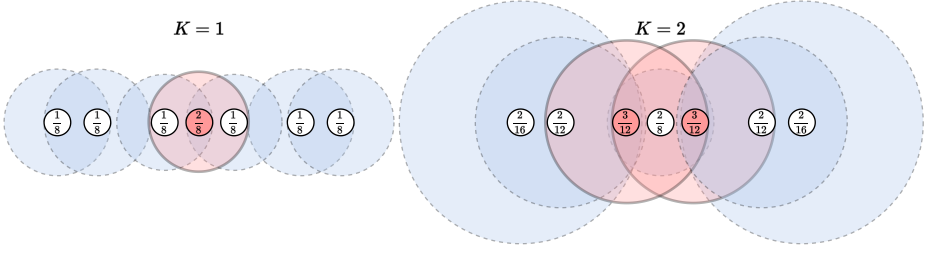


Fig. 2: Visualization of how the notion of sample density, defined as the number of neighbors divided by the volume (see numbers in circles), varies depending on the chosen hyperparameter K . Red indicates the densest samples for each setting of K . As K increases, the density changes and, more importantly, so does the ordering.

Lemma 2. *The expected coverage of a coreset of size $s \leq |\mathcal{T}| - K$ and a given K is*

$$\mathbb{E}_{\mathcal{S} \sim \mathcal{U}(2^{\mathcal{T}})} [\text{coverage}_K(\mathcal{S}, \mathcal{T}) | |\mathcal{S}| = s] = 1 - \prod_{k=0}^K \frac{(|\mathcal{T}| - s - k)}{(|\mathcal{T}| - k)}. \quad (9)$$

Proof.

$$\begin{aligned} \mathbb{E}_{\mathcal{S} \sim \mathcal{U}(2^{\mathcal{T}})} [\text{coverage}_K(\mathcal{S}, \mathcal{T}) | |\mathcal{S}| = s] & \\ &= \frac{1}{|\mathcal{T}|} \sum_{\mathbf{x} \in \mathcal{T}} \mathbb{P}[\exists \mathbf{x}_S \in \mathcal{S} \text{ s.t. } \mathbf{x}_S \in B(\mathbf{x}, \text{NND}_K(\mathbf{x}))] \\ &\stackrel{(i)}{=} 1 - \mathbb{P}[\forall \mathbf{x}_S \in \mathcal{S}, \mathbf{x}_S \notin B(\mathbf{x}_1, \text{NND}_K(\mathbf{x}_1))] \\ &= 1 - \mathbb{P}[S \cap B(\mathbf{x}_1, \text{NND}_K(\mathbf{x}_1)) = \emptyset] \end{aligned} \quad (10)$$

Since by the uniform nature of \mathcal{S} all samples $x \in \mathcal{T}$ are treated equally, we can fix a particular test sample $\mathbf{x}_1 \in \mathcal{T}$ in step (i). The notation \mathbf{x}_1 emphasizes that this sample is now held fixed when we compute $\mathbb{P}[\forall \mathbf{x}_S \in \mathcal{S} : \dots]$. It plays the same role as any other \mathbf{x} in \mathcal{T} . We can reformulate the probability as follows:

Let $Z = (z_1, \dots, z_{|\mathcal{T}|})$ be $|\mathcal{T}|$ non-negative real numbers distributed i.i.d. according to \mathbb{P}_Z . Select $|\mathcal{S}| = s$ many of them uniformly at random, i.e., the expected value is over $\mathcal{S} \sim \mathcal{U}(2^{\mathcal{T}})$. What is the probability that the K smallest entries among Z are not in \mathcal{S} ?

Since the selection is equally likely, we can calculate the probability by counting the ratio of possible selections where the K smallest elements are not selected, which for $|\mathcal{S}| < |\mathcal{T}| - K$ boils down to:

$$\mathbb{P}[\forall \mathbf{x}_S \in \mathcal{S}, \mathbf{x}_S \notin B(\mathbf{x}_1, \text{NND}_K(\mathbf{x}_1))] = \frac{\binom{|\mathcal{T}| - K}{|\mathcal{S}|}}{\binom{|\mathcal{T}|}{|\mathcal{S}|}} = \prod_{k=0}^K \frac{(|\mathcal{T}| - |\mathcal{S}| - k)}{(|\mathcal{T}| - k)}.$$

For $|\mathcal{S}| \geq |\mathcal{T}| - K$ (not interesting for coreset selection), the probability becomes 1.

3.4 Determining the Radius

Figure 3 illustrates how the expected coverage (Equation 9) evolves as K increases under varying pruning levels. We see that the expected coverage tends to rise concavely, indicating diminishing returns once a sufficiently large neighborhood is considered. Higher pruning ratios accentuate this effect, as removing more samples reduces the coverage for a given radius-defining K .

Following this analysis, we repurpose the closed-form expectation in Equation 9 to estimate a suitable value of K for our density calculation under a target coverage. Concretely, for a given coverage goal $\gamma \in (0, 1)$, one can (numerically) invert the expression for assigning K to

$$\min \left\{ K \in \mathbb{N} \left| 1 - \gamma \leq \prod_{k=0}^K \frac{(|\mathcal{T}| - |\mathcal{S}| - k)}{(|\mathcal{T}| - k)} \right. \right\}$$

which finds a suitable K that achieves coverage $_K(\mathcal{S}, \mathcal{T}) \approx \gamma$ under the given conditions. Once this K is determined, we can substitute it back into the density formula in Equation 7 to assign an importance weight to each sample. More details in the appendix.

Notably, the expected coverage in Equation 9 is agnostic to the underlying data and coreset distribution, which means we can calculate it without requiring any training or knowledge about the dataset except its magnitude. In other words, the distance-based counting of neighbors in the set \mathcal{S} (scaled by the chosen K) provides a straightforward training-free importance weighting scheme. This ensures that samples that are more densely surrounded receive greater importance in subsequent pruning.

In summary, by estimating and settling on such a K , we unify coverage and density into a single selection procedure. Specifically, once K is determined from our coverage objective (Equation 9), we compute the K -nearest-neighbor radii for each data sample \mathbf{x}_i . We then greedily select from \mathcal{T} the subset \mathcal{S} of the required size $|\mathcal{S}| = (1 - \alpha) \cdot |\mathcal{T}|$ that maximizes $f_{\text{SubZeroCore}}(\mathcal{S})$ in Equation 7. Owing to the submodularity and monotonicity of the facility location objective, this greedy selection achieves the $(1 - 1/e)$ approximation guarantee (see *Nemhauser et al.* [50]).

Overall, SubZeroCore systematically and effectively reconciles the often competing demands of coverage and density within a single submodular optimization target. By deriving the single hyperparameter K from a closed-form solution, our method achieves a robust and efficient coreset selection without any training overhead, making it practically attractive for scalable deep-learning applications.

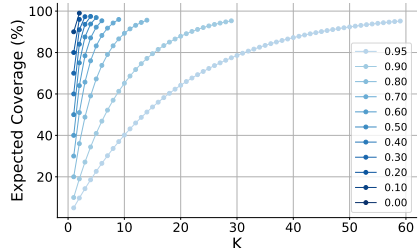


Fig. 3: Expected coverage as a function of K across varying pruning ratios. As K increases, the expected coverage follows a nonlinear trajectory, aligning with the expectation of diminishing returns of additional samples under pruning.

Table 2: Coreset performances on CIFAR-10 with five randomly initialized ResNet-18 [21] models. Without pruning ($\alpha = 0\%$), the model reaches 95.6 ± 0.1 .

Pruning Factor (α)	99.9%	99.5%	99%	95%	90%	80%	70%	60%	50%	40%	10%	Train Signals
Herding [69]	19.8 \pm 2.7	29.2 \pm 2.4	31.1 \pm 2.9	50.7 \pm 1.6	63.1 \pm 3.4	75.2 \pm 1.0	80.8 \pm 1.5	85.4 \pm 1.2	88.4 \pm 0.6	90.9 \pm 0.4	94.4 \pm 0.1	✗
k-Center Greedy [57]	19.9 \pm 0.9	25.3 \pm 0.9	32.6 \pm 1.6	55.6 \pm 2.8	74.6 \pm 0.9	87.3\pm0.2	91.0 \pm 0.3	92.6 \pm 0.2	93.5 \pm 0.5	94.3 \pm 0.2	95.5 \pm 0.2	✗
Forgetting [65]	21.3 \pm 1.2	29.7 \pm 0.3	35.6 \pm 1.0	51.1 \pm 2.0	66.9 \pm 2.0	86.6 \pm 1.0	91.7\pm0.3	93.0\pm0.2	94.1 \pm 0.2	94.6 \pm 0.2	95.4 \pm 0.1	✓
GraNd [53]	14.6 \pm 0.8	17.2 \pm 0.8	18.6 \pm 0.8	28.9 \pm 0.5	41.3 \pm 1.3	71.1 \pm 1.3	88.3 \pm 1.0	93.0\pm0.4	94.8\pm0.1	95.2\pm0.1	95.5 \pm 0.1	✓
CAL [40]	23.1 \pm 1.8	31.7 \pm 0.9	39.7 \pm 3.8	60.8 \pm 1.4	69.7 \pm 0.8	79.4 \pm 0.9	85.1 \pm 0.7	87.6 \pm 0.3	89.0 \pm 0.4	90.9 \pm 0.4	94.7 \pm 0.2	✓
DeepFool [17]	18.7 \pm 0.9	26.4 \pm 1.1	28.3 \pm 0.6	47.7 \pm 3.5	61.2 \pm 2.8	82.7 \pm 0.5	90.8 \pm 0.5	92.9 \pm 0.2	94.4 \pm 0.1	95.6\pm0.1	✓	✓
Craig [42]	19.3 \pm 0.3	29.1 \pm 1.6	32.8 \pm 1.8	42.5 \pm 1.7	59.9 \pm 2.1	78.1 \pm 2.5	90.0 \pm 0.5	92.8 \pm 0.2	94.3 \pm 0.2	94.8 \pm 0.1	95.5 \pm 0.1	✓
GradMatch [29]	17.4 \pm 1.6	27.1 \pm 1.1	27.7 \pm 2.0	41.8 \pm 2.4	55.5 \pm 2.3	78.1 \pm 2.0	89.6 \pm 0.7	92.7 \pm 0.5	94.1 \pm 0.2	94.7 \pm 0.3	95.4 \pm 0.1	✓
Glister [30]	18.4 \pm 1.3	26.5 \pm 0.7	29.4 \pm 1.9	42.1 \pm 1.0	56.8 \pm 1.8	77.2 \pm 2.4	88.8 \pm 0.6	92.7 \pm 0.4	94.2 \pm 0.1	94.8 \pm 0.2	95.5 \pm 0.1	✓
Facility Location	21.0 \pm 1.3	30.3 \pm 1.2	38.1 \pm 1.3	58.8 \pm 2.3	70.9 \pm 1.9	86.6 \pm 0.9	91.2 \pm 0.4	92.9 \pm 0.2	94.3 \pm 0.1	94.7 \pm 0.1	95.5 \pm 0.1	✗
SubZeroCore (ours)	24.0\pm1.9	32.9\pm1.5	39.8\pm1.1	63.9\pm2.0	77.4\pm0.8	87.3\pm0.5	90.8 \pm 0.3	92.5 \pm 0.1	93.2 \pm 0.1	94.1 \pm 0.1	95.3 \pm 0.1	✗

3.5 Implications for Submodularity and Global Coverage

Since the density scores s_j are smaller in sparse regions (where r_j is large) and close to 1 in averagely denser regions (where r_j is small), the weighted objective penalizes the contribution of samples in sparse areas even if they might improve global coverage. Thus, for lower pruning ratios and smaller K , our approach tends to lead to better coreset coverage due to its focus on averagely dense regions, while for higher pruning ratios and higher K , it tends to lead to lower coreset coverage. As a consequence, its focus on data density over data coverage is more profound for high pruning ratios, a property generally favorable for coreset selection [57]. Empirical validation is provided in Table 1.

Table 1: Coverage on CIFAR-10 calculated with respect to the corresponding K -value: Equation 9 with target coverage $\gamma = 0.6$ delivered the K -values 84, 18, 9, 3 for pruning factors 99%, 95%, 90%, 70%, respectively.

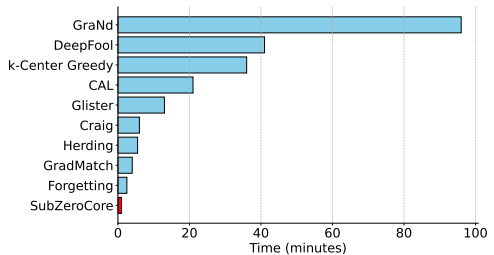
Pruning Factor (α)	99%	95%	90%	70%
Facility Location	56.16	60.36	60.97	65.38
SubZeroCore (ours)	46.77	73.73	80.49	89.03

4 Experiments

This section provides our experiments on CIFAR-10 [34] and ImageNet-1K [14], which evaluates our method SubZeroCore under various aspects, such as overall coreset quality, runtime, and robustness.

4.1 CIFAR-10 Results

Setup. For CIFAR-10, we follow the training protocols of DeepCore [20]. Concretely, we use five ResNet-18 [21] models trained with stochastic gradient descent

**Fig. 4:** Time-Measurement on CIFAR-10. The bar chart compares the selection times (in minutes) of various methods ($\alpha = 0.99$). SubZeroCore (red) significantly outperforms all other methods, requiring only 1 minute, while other techniques take substantially longer due to the prior training phase before pruning.

(SGD) on coresets for 200 epochs, using a batch size of 128, an initial learning rate of 0.1 with cosine annealing, momentum 0.9, and weight decay 5×10^{-4} and evaluate the trained model on the standard CIFAR-10 test set. We subselect multiple fractions from the full training set, whose performance we treat as an approximate upper bound. Data augmentation includes a random 4-pixel padding followed by cropping to 32×32 , and random horizontal flips.

Main Results. In Table 2, we show how SubZeroCore compares against existing coreset selection methods on CIFAR-10 under various pruning ratios (from 10% up to 99.9%). Notably, our approach closely matches all baselines for lower pruning rates (70% and below), or consistently outperforms for pruning ratios above 70%, especially for ultra-scarce settings. More details on complexity and additional cross-architecture evaluations (VGG-16 [58], InceptionNetV3 [64], WRN-16-8 [75], and ResNet-50 [21]) can found in the appendix. Moreover, we achieve all results while being notably faster due to our training-free setup, as shown in Figure 4.

Robustness. To assess the stability of our coreset selection method under label noise or malicious relabeling, we follow a poisoning protocol similar to that in Zhang et al. [76]. Specifically, we randomly relabel 10% of CIFAR-10 training examples to incorrect classes, thereby introducing a form of data poisoning. We then run each coreset selection method on this poisoned dataset, subsampling different fractions. The relative accuracy change (compared to no poisoning) is shown in Figure 5. We observe that our method SubZeroCore demonstrates profound robustness among all baselines, effectively mitigating the detrimental effects of relabeling noise (i.e., mislabeled data). Notably, its performance remains superior to the standard facility location method. In fact, by incorporating the density-weighted mechanism, our method downweights outlier samples (where mislabeled or corrupted data often lie), yielding a stable coreset even under harsh poisoning scenarios. Such improvements highlight that the density weighting scheme is not only beneficial for standard data selection but also enhances resilience to adversarial or noisy training conditions.

4.2 ImageNet-1K Results

Setup. For our ImageNet-1K experiments, we train three ResNet-18 models on the selected coresets using a batch size of 256 for 200 epochs. Training images are randomly cropped and resized to 224×224 , and horizontal flipping is applied with a probability of 50%. All other experimental settings and training hyperparameters are identical to those used in our CIFAR-10 experiments.

Main Results. As shown in Table 3, SubZeroCore consistently ranks among the top-performing methods across all pruning levels, outperforming nearly all training-based approaches. In particular, it matches or slightly exceeds Forgetting at higher pruning ratios and outperforms Craig, GradMatch, and CAL most of the time. Notably, SubZeroCore achieves this performance without any model-specific training.

Table 3: Coreset selection performances on ImageNet-1K. We train randomly initialized ResNet-18 on the pruned subsets produced by various methods and test on the real ImageNet test set. DeepFool and GraNd were omitted due to their significant memory requirements and runtime.

Pruning Factor (α)	90%	80%	70%	60%	50%	0%	Train Signals
Herdling [69]	29.17 \pm 0.23	41.26 \pm 0.43	48.71 \pm 0.23	54.65 \pm 0.07	58.92 \pm 0.19	69.52 \pm 0.45	✗
k-Center Greedy [57]	48.11 \pm 0.29	59.06 \pm 0.22	62.91 \pm 0.22	64.93 \pm 0.22	66.04 \pm 0.05	69.52 \pm 0.45	✗
Forgetting [65]	55.31\pm0.07	60.36 \pm 0.12	62.45 \pm 0.11	63.97 \pm 0.01	65.06 \pm 0.02	69.52 \pm 0.45	✓
CAL [40]	46.08 \pm 0.10	53.71 \pm 0.19	58.11 \pm 0.13	61.17 \pm 0.06	63.67 \pm 0.28	69.52 \pm 0.45	✓
Craig [42]	51.39 \pm 0.13	59.33 \pm 0.22	62.72 \pm 0.13	64.96 \pm 0.00	66.29 \pm 0.00	69.52 \pm 0.45	✓
GradMatch [29]	47.57 \pm 0.32	56.29 \pm 0.31	60.62 \pm 0.28	64.40 \pm 0.33	65.02 \pm 0.50	69.52 \pm 0.45	✓
Glister [30]	47.02 \pm 0.29	55.93 \pm 0.17	60.38 \pm 0.17	62.86 \pm 0.07	65.07 \pm 0.08	69.52 \pm 0.45	✓
Facility Location	52.49 \pm 0.19	60.06 \pm 0.11	63.05 \pm 0.06	65.24 \pm 0.04	66.05 \pm 0.07	69.52 \pm 0.45	✗
SubZeroCore (ours)	54.01 \pm 0.14	60.78 \pm 0.05	63.35 \pm 0.11	65.32 \pm 0.04	66.14 \pm 0.07	69.52 \pm 0.45	✗

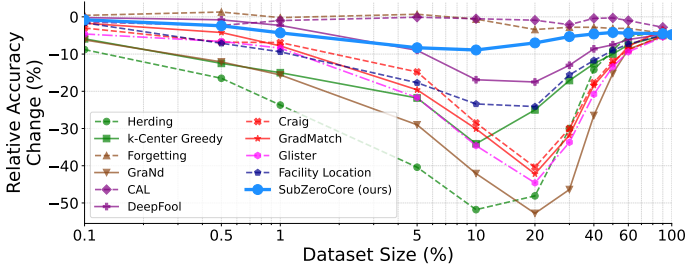


Fig. 5: Relative robustness of coreset selection methods on CIFAR-10 with 10% corrupted labels. SubZeroCore demonstrates strong robustness (among top-3 methods with CAL and Forgetting), even outperforming facility location, the method it builds upon.

4.3 Impact of Target Coverage

Recall that SubZeroCore has only one hyperparameter, namely the desired coverage level $\gamma \in (0, 1)$ for Equation 9. We conduct an ablation study (see Figure 6) by varying γ and then measuring the final test accuracy under different pruning ratios. We observe that, for moderate or low pruning rates, SubZeroCore remains relatively insensitive to the exact choice of γ . However, at high pruning rates, different γ -values lead to significant gaps in final accuracy. Through this exploration, we find that a target coverage of $\gamma \approx 0.60$ offers the best trade-off between robust performance and insensitiv-

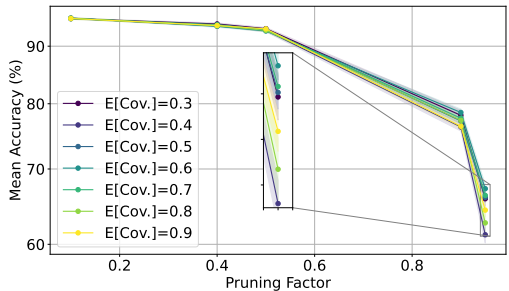


Fig. 6: Expected coverage (γ) ablation on CIFAR-10. While for lower pruning ratios, the setting of γ does not have a notable impact, it significantly influences the outcome for higher pruning ratios. We identify a target coverage of 0.6 as the best option.

ity to pruning levels. Consequently, we adopted $\gamma = 0.60$ in our reported CIFAR-10 and ImageNet-1K experiments.

5 Limitations

SubZeroCore may yield less meaningful estimates in the regime where $|\mathcal{T}|$ is small, although our coverage derivation in Equation 9 cleanly holds for sufficiently large datasets. Mathematically, the closed-form expression hinges on selecting $|\mathcal{S}|$ subsets from a larger pool $|\mathcal{T}|$. When $|\mathcal{T}|$ is only marginally bigger than $|\mathcal{S}|$, the binomial coefficients $\binom{|\mathcal{T}|-K}{|\mathcal{S}|}$ and $\binom{|\mathcal{T}|}{|\mathcal{S}|}$ can be extremely sensitive to small changes in $|\mathcal{S}|$ or K . Consequently, small-sample effects can inflate (or deflate) the predicted coverage in ways that do not generalize outside the combinatorial assumptions underlying the derivation. Thus, if the dataset itself is tiny (e.g., tens or hundreds of samples), then the notion of “expected coverage” over all possible subsets becomes so discretized that it no longer provides a stable yardstick for coverage-driven coreset selection. We recommend a direct check of coverage in such low-data scenarios (though it remains questionable whether coreset selection is even necessary in extremely small datasets), rather than relying on the asymptotic-style expression in Equation 9.

6 Related Work

Coreset selection has been explored from multiple angles. On the training-based front, various importance-scoring heuristics like the forgetting score [65], AUM [54], and EL2N [53] estimate how much a training example influences model parameters or loss dynamics, then keep only those deemed most essential. Other methods like GraNd [53] or GradMatch [29] exploit the gradients during training, while DeepFool [17] or CAL [40] leverage an approximation of the decision boundary during training. However, computing these metrics usually demands full or partial training rounds and can be computationally heavy. Regarding training-free methods, k-means clustering or greedy k-center have been proposed to directly achieve good coverage in feature space [57, 61], but usually underperform if the embedded feature space is not trained on the full dataset like in our experiments. Also, their sole focus is pure coverage, making it highly effective at covering the entire data space but also sensitive to outliers, as it will prioritize isolated points to reduce the worst-case distance.

Beyond coreset selection specifically, data subsets or proxy selection also appears in active learning, where approaches like BADGE [3] or BatchBALD [31] repeatedly query diverse, high-uncertainty examples to improve a model at each round. Although active learning shares the goal of sampling efficiently, it typically relies on sequential label querying and repeated model updates, which differ from our training-free, model-agnostic setting. Another relevant line of research pertains to coreset constructions for *classical clustering* problems (e.g., k-means), where theoretical guarantees can be derived through importance sampling or

similar randomization strategies [5, 10, 12, 18]. These techniques, however, leverage the geometry of clustering objectives rather than classification or representation-learning signals, making them less adaptable to broad deep-learning tasks.

7 Conclusion & Future Work

In this paper, we introduced SubZeroCore, a novel coreset selection method that elegantly unifies density and coverage into a single submodular optimization objective without requiring any training signals. Unlike existing training-based methods, SubZeroCore operates sufficiently in a purely geometric-based setting and significantly reduces computational overhead. Moreover, we reduced the number of hyperparameters for the coreset selection to one, whereas existing methods rely on good model-specific choices. Our theoretical analysis, supported by extensive experiments on CIFAR-10 and ImageNet-1K, demonstrates that SubZeroCore not only maintains competitive accuracy at lower pruning rates but also outperforms state-of-the-art results at high pruning rates. Moreover, we have shown that our density-based weighting scheme naturally provides robustness against label noise, making it suitable for real-world scenarios with potentially corrupted or noisy data.

In conclusion, SubZeroCore presents a meaningful step forward in making large-scale coreset selection more resource-efficient and environmentally sustainable. Future work includes extending the framework to dynamic data streams, further broadening its applicability. Moreover, one could introduce an additional power on the weights to explicitly control between density and coverage.

References

1. Abbas, A., Rusak, E., Tirumala, K., Brendel, W., Chaudhuri, K., Morcos, A.S.: Effective pruning of web-scale datasets based on complexity of concept clusters. arXiv preprint arXiv:2401.04578 (2024)
2. Agarwal, P.K., Har-Peled, S., Varadarajan, K.R., et al.: Geometric approximation via coresets. *Combinatorial and computational geometry* **52**(1), 1–30 (2005)
3. Ash, J.T., Zhang, C., Krishnamurthy, A., Langford, J., Agarwal, A.: Deep batch active learning by diverse, uncertain gradient lower bounds. arXiv preprint arXiv:1906.03671 (2019)
4. Bachem, O., Lucic, M., Krause, A.: Practical coreset constructions for machine learning. arXiv preprint arXiv:1703.06476 (2017)
5. Bahmani, B., Moseley, B., Vattani, A., Kumar, R., Vassilvitskii, S.: Scalable k-means++. arXiv preprint arXiv:1203.6402 (2012)
6. Bengio, S., Dembczynski, K., Joachims, T., Kloft, M., Varma, M.: Extreme classification (dagstuhl seminar 18291). In: Dagstuhl Reports. vol. 8. Schloss Dagstuhl-Leibniz-Zentrum fuer Informatik (2019)
7. Bérczi, K., Bérczi-Kovács, E.R., Lorincz, A., Milacski, Z.: Facility location functions are deep submodular functions (2019)
8. Bhalerao, M.M.: On Fine-Tuning Submodular Functions for Data Subset Selection. Master’s thesis, University of Washington (2024)

9. Borsos, Z., Mutny, M., Krause, A.: Coresets via bilevel optimization for continual learning and streaming. *NeurIPS* **33**, 14879–14890 (2020)
10. Caron, M., Bojanowski, P., Joulin, A., Douze, M.: Deep clustering for unsupervised learning of visual features. In: *ECCV*. pp. 132–149 (2018)
11. Chen, Y., Wang, Y., Su, J., et al.: Unified framework for coreset selection and dataset distillation by distribution matching. Available at SSRN (8 2024), https://ssrn.com/abstract_id=4935536
12. Cohen-Addad, V., Draganov, A., Russo, M., Saulpic, D., Schwiegelshohn, C.: A tight vc-dimension analysis of clustering coresets with applications. In: *Proceedings of the 2025 Annual ACM-SIAM Symposium on Discrete Algorithms (SODA)*. pp. 4783–4808. SIAM (2025)
13. Csiba, D., Richtárik, P.: Importance sampling for minibatches. *The Journal of Machine Learning Research* **19**(1), 962–982 (2018)
14. Deng, J., Dong, W., Socher, R., Li, L.J., Li, K., Fei-Fei, L.: Imagenet: A large-scale hierarchical image database. In: *CVPR*. pp. 248–255. Ieee (2009)
15. Ding, Q., Liang, Z., Wang, L., Wang, Y., Yang, J.: Not all patches are equal: Hierarchical dataset condensation for single image super-resolution. *IEEE Signal Processing Letters* (2023)
16. Dou, J., Yu, C., Jiang, Y., Wang, Z., Fu, Q., Han, Y.: Coreset optimization by memory constraints, for memory constraints (10 2023)
17. Ducoffe, M., Precioso, F.: Adversarial active learning for deep networks: a margin based approach. *arXiv preprint arXiv:1802.09841* (2018)
18. Feldman, D.: Core-sets: Updated survey. *Sampling techniques for supervised or unsupervised tasks* pp. 23–44 (2020)
19. Ganguli, D., Hernandez, D., Lovitt, L., Askell, A., Bai, Y., Chen, A., Conerly, T., Dassarma, N., Drain, D., Elhage, N., et al.: Predictability and surprise in large generative models. In: *2022 ACM Conference on Fairness, Accountability, and Transparency* (2022)
20. Guo, C., Zhao, B., Bai, Y.: Deepcore: A comprehensive library for coreset selection in deep learning. In: *International Conference on Database and Expert Systems Applications*. pp. 181–195. Springer (2022)
21. He, K., Zhang, X., Ren, S., Sun, J.: Deep residual learning for image recognition. In: *CVPR*. pp. 770–778 (2016)
22. Huang, Y., Yuan, X., Wang, H., Du, Y.: Coreset selection can accelerate quantum machine learning models with provable generalization. *Physical Review Applied* **22**(1), 014074 (2024)
23. Iyer, R., Jegelka, S., Bilmes, J.: Fast semidifferential-based submodular function optimization. In: *ICML*. pp. 855–863. PMLR (2013)
24. Iyer, R., Khargoankar, N., Bilmes, J., Asanani, H.: Submodular combinatorial information measures with applications in machine learning. In: *Algorithmic Learning Theory*. pp. 722–754. PMLR (2021)
25. Iyer, R.K., Bilmes, J.A.: Submodular optimization with submodular cover and submodular knapsack constraints. *NeurIPS* **26** (2013)
26. Karanam, A., Killamsetty, K., Kokel, H., Iyer, R.: Orient: Submodular mutual information measures for data subset selection under distribution shift. *NeurIPS* **35**, 31796–31808 (2022)
27. Katharopoulos, A., Fleuret, F.: Not all samples are created equal: Deep learning with importance sampling. In: *ICML*. pp. 2525–2534. PMLR (2018)
28. Khandel, P., Yates, A., Varbanescu, A.L., De Rijke, M., Pimentel, A.: Distillation vs. sampling for efficient training of learning to rank models. In: *Proceedings of the*

- 2024 ACM SIGIR International Conference on Theory of Information Retrieval. pp. 51–60 (2024)
29. Killamsetty, K., Durga, S., Ramakrishnan, G., De, A., Iyer, R.: Grad-match: Gradient matching based data subset selection for efficient deep model training. In: ICML. pp. 5464–5474. PMLR (2021)
 30. Killamsetty, K., Sivasubramanian, D., Ramakrishnan, G., Iyer, R.: Glistner: Generalization based data subset selection for efficient and robust learning. In: AAAI. vol. 35, pp. 8110–8118 (2021)
 31. Kirsch, A., Van Amersfoort, J., Gal, Y.: Batchbald: Efficient and diverse batch acquisition for deep bayesian active learning. *NeurIPS* **32** (2019)
 32. Koh, P.W., Liang, P.: Understanding black-box predictions via influence functions. In: ICML. pp. 1885–1894. PMLR (2017)
 33. Kothawade, S., Kaushal, V., Ramakrishnan, G., Bilmes, J., Iyer, R.: Submodular mutual information for targeted data subset selection. *arXiv preprint arXiv:2105.00043* (2021)
 34. Krizhevsky, A., Hinton, G., et al.: Learning multiple layers of features from tiny images (2009)
 35. Laribi, N., Gaceb, D., Touazi, F., Rezoug, A.: Application of dataset pruning and dynamic transfer learning on vision transformers for mgmt prediction on brain mri images. In: 2024 1st International Conference on Innovative and Intelligent Information Technologies (IC3IT). pp. 1–6. IEEE (2024)
 36. Lee, S., Chung, J., Yu, Y., Kim, G., Breuel, T., Chechik, G., Song, Y.: Acav100m: Automatic curation of large-scale datasets for audio-visual video representation learning. In: CVPR. pp. 10274–10284 (2021)
 37. Lim, C.L., Moffat, A., Wirth, A.: Lazy and eager approaches for the set cover problem. In: Proceedings of the Thirty-Seventh Australasian Computer Science Conference-Volume 147. pp. 19–27 (2014)
 38. Lundberg, S.M., Lee, S.I.: A unified approach to interpreting model predictions. *NeurIPS* **30** (2017)
 39. Luo, Y., Zhao, S., Wu, H., Lu, Z.: Dual-enhanced coreset selection with class-wise collaboration for online blurry class incremental learning. In: CVPR. pp. 23995–24004 (2024)
 40. Margatina, K., Vernikos, G., Barrault, L., Aletras, N.: Active learning by acquiring contrastive examples. *arXiv preprint arXiv:2109.03764* (2021)
 41. Marion, M., Üstün, A., Pozzobon, L., Wang, A., Fadaee, M., Hooker, S.: When less is more: Investigating data pruning for pretraining llms at scale. *arXiv preprint arXiv:2309.04564* (2023)
 42. Mirzasoleiman, B., Bilmes, J., Leskovec, J.: Coresets for data-efficient training of machine learning models. In: ICML. pp. 6950–6960. PMLR (2020)
 43. Morgan, F.: Geometric measure theory: a beginner’s guide. Academic press (2016)
 44. Moser, B., Raue, F., Hees, J., Dengel, A.: Less is more: Proxy datasets in nas approaches. In: CVPR. pp. 1953–1961 (2022)
 45. Moser, B.B., Raue, F., Dengel, A.: A study in dataset pruning for image super-resolution. In: International Conference on Artificial Neural Networks. pp. 351–363. Springer (2024)
 46. Moser, B.B., Raue, F., Nauen, T.C., Frolov, S., Dengel, A.: Distill the best, ignore the rest: Improving dataset distillation with loss-value-based pruning. *arXiv preprint arXiv:2411.12115* (2024)
 47. Moser, B.B., Shanbhag, A.S., Frolov, S., Raue, F., Folz, J., Dengel, A.: A coreset selection of coreset selection literature: Introduction and recent advances. *arXiv preprint arXiv:2505.17799* (2025)

48. Na, B., Mok, J., Choe, H., Yoon, S.: Accelerating neural architecture search via proxy data. arXiv preprint arXiv:2106.04784 (2021)
49. Naeem, M.F., Oh, S.J., Uh, Y., Choi, Y., Yoo, J.: Reliable fidelity and diversity metrics for generative models. In: ICML. pp. 7176–7185. PMLR (2020)
50. Nemhauser, G.L., Wolsey, L.A., Fisher, M.L.: An analysis of approximations for maximizing submodular set functions—i. Mathematical programming **14**, 265–294 (1978)
51. Nguyen, C.V., Li, Y., Bui, T.D., Turner, R.E.: Variational continual learning. arXiv preprint arXiv:1710.10628 (2017)
52. Nogueira, S., Sechidis, K., Brown, G.: On the stability of feature selection algorithms. Journal of Machine Learning Research **18**(174), 1–54 (2018)
53. Paul, M., Ganguli, S., Dziugaite, G.K.: Deep learning on a data diet: Finding important examples early in training. NeurIPS **34**, 20596–20607 (2021)
54. Pleiss, G., Zhang, T., Elenberg, E., Weinberger, K.Q.: Identifying mislabeled data using the area under the margin ranking. NeurIPS **33**, 17044–17056 (2020)
55. Qu, F., Erfani, S.M., Usman, M.: Performance analysis of coreset selection for quantum implementation of k-means clustering algorithm. arXiv preprint arXiv:2206.07852 (2022)
56. Ren, M., Zeng, W., Yang, B., Urtasun, R.: Learning to reweight examples for robust deep learning. In: ICML. pp. 4334–4343. PMLR (2018)
57. Sener, O., Savarese, S.: Active learning for convolutional neural networks: A core-set approach. arXiv preprint arXiv:1708.00489 (2017)
58. Simonyan, K., Zisserman, A.: Very deep convolutional networks for large-scale image recognition. arXiv preprint arXiv:1409.1556 (2014)
59. Sivasubramanian, D., Nagalapatti, L., Iyer, R., Ramakrishnan, G.: Gradient coreset for federated learning. In: CVPR. pp. 2648–2657 (2024)
60. Song, L., Zhang, J., Yang, T., Goto, M.: Adaptive ranking-based sample selection for weakly supervised class-imbalanced text classification. arXiv preprint arXiv:2210.03092 (2022)
61. Sorscher, B., Geirhos, R., Shekhar, S., Ganguli, S., Morcos, A.: Beyond neural scaling laws: beating power law scaling via data pruning. NeurIPS **35**, 19523–19536 (2022)
62. Svitkina, Z., Fleischer, L.: Submodular approximation: Sampling-based algorithms and lower bounds. SIAM Journal on Computing **40**(6), 1715–1737 (2011)
63. Swayamdipta, S., Schwartz, R., Lourie, N., Wang, Y., Hajishirzi, H., Smith, N.A., Choi, Y.: Dataset cartography: Mapping and diagnosing datasets with training dynamics. arXiv preprint arXiv:2009.10795 (2020)
64. Szegedy, C., Vanhoucke, V., Ioffe, S., Shlens, J., Wojna, Z.: Rethinking the inception architecture for computer vision. In: CVPR. pp. 2818–2826 (2016)
65. Toneva, M., Sordoni, A., Combes, R.T.d., Trischler, A., Bengio, Y., Gordon, G.J.: An empirical study of example forgetting during deep neural network learning. arXiv preprint arXiv:1812.05159 (2018)
66. Wang, T., Zhu, J.Y., Torralba, A., Efros, A.A.: Dataset distillation. arXiv preprint arXiv:1811.10959 (2018)
67. Wei, K., Iyer, R., Bilmes, J.: Submodularity in data subset selection and active learning. In: ICML. PMLR (2015)
68. Wei, K., Liu, Y., Kirchhoff, K., Bartels, C., Bilmes, J.: Submodular subset selection for large-scale speech training data. In: 2014 IEEE International Conference on Acoustics, Speech and Signal Processing (ICASSP). pp. 3311–3315. IEEE (2014)
69. Welling, M.: Herding dynamical weights to learn. In: ICML. pp. 1121–1128 (2009)

70. Xiao, L., Liu, S., He, Y., Wang, X.: Rethinking large-scale dataset compression: Shifting focus from labels to images. arXiv preprint arXiv:2502.06434 (2025)
71. Xue, Y., Chen, X., Li, T., Jiang, S.H.C.: Near-optimal quantum coreset construction algorithms for clustering. In: ICML. pp. 38881–38912. PMLR (2023)
72. Yang, R., Su, L.: Data-efficient trajectory prediction via coreset selection. arXiv preprint arXiv:2409.17385 (2024)
73. Yao, P., Liao, C., Jia, J., Tan, J., Chen, B., Song, C., Zhang, D.: Asp: Automatic selection of proxy dataset for efficient automl. arXiv preprint arXiv:2310.11478 (2023)
74. Yoon, J., Madaan, D., Yang, E., Hwang, S.J.: Online coreset selection for rehearsal-based continual learning. arXiv preprint arXiv:2106.01085 (2021)
75. Zagoruyko, S., Komodakis, N.: Wide residual networks. arXiv preprint arXiv:1605.07146 (2016)
76. Zhang, C., Bengio, S., Hardt, M., Recht, B., Vinyals, O.: Understanding deep learning (still) requires rethinking generalization. Communications of the ACM **64**(3), 107–115 (2021)
77. Zheng, H., Liu, R., Lai, F., Prakash, A.: Coverage-centric coreset selection for high pruning rates. ICLR (2022)

A Connecting Submodularity to Generalization

In this section, we elaborate on how submodular optimization, specifically through maximizing the facility location function, is inherently connected to generalization performance.

Intuitively, the submodular facility location function encourages the selection of representative and diverse subsets by maximizing the similarity coverage of the entire dataset. Such coverage implies that selected points efficiently span the data manifold, reducing redundancy and increasing representativeness. To formalize this intuition, consider the concept of empirical Rademacher complexity, which quantifies the capacity of a function class to fit random labels and thus directly relates to generalization performance:

Lemma 3 (Informal connection to generalization). *Given a data distribution P , and a submodular coverage function $f(\mathcal{S})$ optimized by greedy submodular maximization to achieve at least a $(1 - 1/e)$ approximation, the resulting coreset $\mathcal{S}_{\text{greedy}}$ provides a reduced empirical Rademacher complexity compared to randomly selected subsets of the same size. Consequently, this implies improved expected generalization bounds. Formally,*

$$\mathbb{E}_{\mathbf{x}, y \sim P}[\mathcal{L}(\mathbf{x}, y; \mathcal{S}_{\text{greedy}})] \leq \mathbb{E}_{\mathbf{x}, y \sim P}[\mathcal{L}(\mathbf{x}, y; \mathcal{S}_{\text{random}})] - \Delta, \quad (11)$$

where $\Delta \geq 0$ quantifies the expected gain in generalization due to better coverage.

While a rigorous theoretical derivation of Δ depends on specific assumptions about the data manifold and similarity measures, the conceptual linkage established here supports the observed empirical improvements in generalization for SubZeroCore.

B Density-Weighted Submodularity and Robustness

This section discusses the theoretical reasoning behind why incorporating density weighting within the submodular selection improves robustness to noise and corrupted labels.

The key theoretical intuition is that emphasizing density inherently focuses the coresset selection on regions of the data manifold with greater local consensus. Points residing in densely populated regions are more likely to reflect stable underlying decision boundaries, making them robust to label perturbations and noise.

Lemma 4 (Informal connection to robustness). *Given a density-weighted submodular function defined as*

$$f_{\text{SubZeroCore}}(\mathcal{S}) = \sum_{i \in \mathcal{T}} \max_{j \in \mathcal{S}} (s_j \cdot \text{sim}(\mathbf{x}_i, \mathbf{x}_j)), \quad (12)$$

where s_j are density-based weights favoring dense regions, the resulting selected coresset exhibits increased robustness to mislabeled data compared to subsets selected without density weighting. Specifically, the probability that an outlier or noisy label significantly influences the subset decreases substantially:

$$P(\mathbf{x}_{\text{outlier}} \in \mathcal{S}_{\text{greedy}}) \leq P(\mathbf{x}_{\text{outlier}} \in \mathcal{S}_{\text{non-density}}), \quad (13)$$

where equality only holds in the trivial case of uniformly dense data.

This theoretical viewpoint aligns well with empirical observations in our experiments, providing a conceptual rationale for the robustness benefits observed with SubZeroCore.

C Numerical Inversion of Coverage

To efficiently determine the optimal neighborhood size K given a desired coverage level γ , we implemented a numerical inversion. Basically, it Below we provide the corresponding Python implementation directly extracted from our codebase:

```
def find_k_for_coverage(M, N, c):
    k = 0
    coverage = 0.0
    numerator = 1.0
    denominator = 1.0
    while coverage < c and k < N - M - 1:
        k += 1
        numerator *= (N - M - k)
        denominator *= (N - k)
        coverage = 1.0 - numerator / denominator
    return k
```

D SubZeroCore Algorithm

Algorithm 1 SubZeroCore Selection Procedure

```

1: Input: Dataset  $\mathcal{T} = \{(\mathbf{x}_i, y_i)\}_{i=1}^N$ , pruning ratio  $\alpha \in (0, 1)$ , coverage target  $\gamma \in (0, 1)$ ,
   similarity measure  $\text{sim}(\cdot, \cdot)$ 
2: Output: Coreset  $\mathcal{S}$ , with  $|\mathcal{S}| = (1 - \alpha)|\mathcal{T}|$ 
3: // Compute subset size:
4:  $s \leftarrow (1 - \alpha) \cdot |\mathcal{T}|$ 
5: // Determine optimal  $K$  via numerical inversion (given coverage  $\gamma$ ):
6:  $K \leftarrow \min \left\{ K \in \mathbb{N} \mid 1 - \gamma \leq \prod_{k=0}^K \frac{(|\mathcal{T}| - s - k)}{|\mathcal{T}| - k} \right\}$ 
7: // For each  $\mathbf{x}_i \in \mathcal{T}$ , compute radius:
8:  $r_i \leftarrow \text{NND}_K(\mathbf{x}_i)$ 
9: // Compute empirical mean and standard deviation of radii:
10:  $\mu \leftarrow \frac{1}{|\mathcal{T}|} \sum_{i=1}^{|\mathcal{T}|} r_i$ ,  $\sigma \leftarrow \sqrt{\frac{1}{|\mathcal{T}|} \sum_{i=1}^{|\mathcal{T}|} (r_i - \mu)^2}$ 
11: // For each  $\mathbf{x}_i \in \mathcal{T}$ , compute density-based weights:
12:  $s_i \leftarrow \exp \left( -\frac{(r_i - \mu)^2}{2\sigma^2} \right)$ 
13:
14: // Greedily select the coreset by maximizing the weighted facility location:
15: // Initialize
16:  $\mathcal{S} \leftarrow \emptyset$ 
17: while  $|\mathcal{S}| < s$  do
18:   // Select next element according to:
19:    $\mathbf{x}^* \leftarrow \arg \max_{\mathbf{x}_j \in \mathcal{T} \setminus \mathcal{S}} \sum_{\mathbf{x}_i \in \mathcal{T}} \max_{\mathbf{x}_k \in \mathcal{S} \cup \{\mathbf{x}_j\}} s_k \cdot \text{sim}(\mathbf{x}_i, \mathbf{x}_k)$ 
20:   // Update:
21:    $\mathcal{S} \leftarrow \mathcal{S} \cup \{\mathbf{x}^*\}$ 
22: end while
23: return  $\mathcal{S}$ 

```

E Complexity Analysis of SubZeroCore

We provide a comprehensive runtime and space complexity analysis for the SubZeroCore algorithm. Below, let:

- N denote the total number of samples in the dataset,
- C denote the number of classes,
- $N_C \approx \frac{N}{C}$ denote the average number of samples per class,
- d denote the dimensionality of the embeddings (e.g., 2048 for Inception v3),
- M denote the coreset size per class (target subset size).

E.1 Runtime Complexity

SubZeroCore has four main computational steps:

1. *Embedding Extraction.* Each embedding is computed via a single forward pass through a pretrained model, resulting in complexity:

$$\mathcal{O}(N \cdot d).$$

2. *Numerical Inversion (Finding K for Coverage).* The numerical inversion (implemented by a simple linear search in practice) has negligible complexity as $K \ll N_C$:

$$\mathcal{O}(K).$$

3. *Computing Radii and Density Scores.* This involves pairwise distance calculations within each class:

$$\mathcal{O}(N_C^2 \cdot d).$$

Computing density scores (mean and standard deviation) adds only a linear term, thus the complexity is dominated by pairwise distance calculation.

4. *Greedy Facility Location Selection.* The greedy selection iterates M times, with each iteration recomputing marginal gains for N_C candidates:

$$\mathcal{O}(M \cdot N_C^2).$$

Summarizing all the steps above, the runtime complexity per class is:

$$\mathcal{O}(N_C^2 \cdot d + M \cdot N_C^2) \approx \mathcal{O}(N_C^2 \cdot d),$$

as typically, $M \ll d$. Thus, global complexity (over all classes) is approximately:

$$\mathcal{O}\left(\frac{N^2 \cdot d}{C}\right).$$

E.2 Space Complexity

SubZeroCore requires storing embeddings and pairwise similarity matrices:

- Embedding storage: $\mathcal{O}(N \cdot d)$,
- Pairwise similarity matrix storage per class: $\mathcal{O}(N_C^2)$.

Thus, the overall memory complexity per class is dominated by the similarity matrix:

$$\mathcal{O}(N_C^2).$$

E.3 When Training-Signal-Based Methods Can Have Lower Complexity

While SubZeroCore benefits significantly from not requiring any model training, there exist specific scenarios where training-signal-based coreset selection methods may exhibit lower computational complexity:

- **Pre-trained Models or Available Gradients:** If the embedding model or gradient signals are already computed as part of a previous training phase or available from prior runs, methods utilizing these signals (e.g., gradient-based selection or forgetting-based methods) can leverage existing computations to significantly reduce incremental complexity. In these cases, complexity reduces to near-linear in the dataset size.
- **Partial or Incremental Training:** Methods that rely on incremental updates of model parameters, rather than full model retraining, can substantially reduce computational overhead compared to the quadratic complexity involved in calculating pairwise distances or similarities used in SubZeroCore.
- **Small Model Architectures:** For simpler or highly optimized models where obtaining training signals (such as gradients or loss values) can be efficiently computed, training-based methods may become less computationally demanding compared to the quadratic scaling of SubZeroCore.

Therefore, SubZeroCore is generally preferable in large-scale, training-free scenarios or settings where training signals are expensive or unavailable. In contrast, training-signal-based methods could become favorable under conditions outlined above.

F Considerations for Embedding Networks in Specialized Domains

While SubZeroCore fundamentally operates as a training-free coreset selection method, its effectiveness hinges on the quality and suitability of the underlying embedding representation. Throughout our experiments on standard datasets such as CIFAR-10 and ImageNet-1K, we observed negligible performance differences across widely used pre-trained feature extractors like ResNet-18, InceptionNetV3, or VGG. This consistency suggests that SubZeroCore is mainly agnostic to these popular embedding models.

However, for highly specialized datasets or unique domain-specific applications (i.e., medical imaging, remote sensing, or multi-modal data), the choice of embedding network may significantly influence the quality of the selected coreset. Such specialized datasets often present distinct characteristics, such as unique feature distributions, intricate semantic relationships, or uncommon modalities that generic pre-trained embeddings may not adequately capture. In these cases, training a specialized embedding network tailored explicitly for the target domain or task could become necessary to achieve optimal coreset selection performance.

G Hardware & Software Details

All experiments were conducted on a workstation equipped with an NVIDIA RTX A6000 GPU (48GB VRAM) using PyTorch 1.10.1 with torchvision 0.11.2 for DeepCore.

H Datasets

We conduct experiments on two widely adopted image classification datasets: CIFAR-10 and ImageNet-1K. Both datasets have the following properties.

- **CIFAR-10** consists of 50,000 training and 10,000 test images across 10 classes. Each image has a resolution of 32×32 pixels. The dataset provides a balanced, compact benchmark for testing coreset selection performance under high pruning ratios.
- **ImageNet-1K** is a large-scale dataset with 1,281,167 training and 50,000 validation images from 1,000 object categories. Following standard coreset evaluation practices, we resize all images to 224×224 resolution for training and testing unless otherwise noted.

I Additional Cross-Architecture Evaluations

Table 4: Coreset selection performances on CIFAR-10 with five randomly initialized VGG-16 models. The best results are marked in bold.

Fraction ($1 - \alpha$)	0.1%	0.5%	1%	5%	10%	20%	30%	40%	50%	60%	90%	100%
Herding	11.6 \pm 1.2	12.7 \pm 0.6	16.0 \pm 3.9	54.1 \pm 3.1	66.0 \pm 3.5	71.5 \pm 1.5	78.3 \pm 1.0	80.9 \pm 0.5	85.7 \pm 1.5	88.2 \pm 0.7	93.2 \pm 0.3	94.3 \pm 0.0
k-Center Greedy	12.3 \pm 1.0	14.5 \pm 2.9	14.7 \pm 1.3	38.7 \pm 12.0	75.6 \pm 1.3	85.5 \pm 0.3	89.0 \pm 0.4	91.0 \pm 0.2	91.8 \pm 0.3	92.7 \pm 0.2	94.1 \pm 0.1	94.3 \pm 0.0
Forgetting	12.5 \pm 0.8	13.8 \pm 2.8	25.6\pm4.3	55.9 \pm 1.3	75.2 \pm 1.4	86.2 \pm 0.2	89.0 \pm 0.2	91.3 \pm 0.2	91.9 \pm 0.2	92.8 \pm 0.0	94.1 \pm 0.2	94.3 \pm 0.0
GraNd	11.7 \pm 0.6	12.5 \pm 0.0	16.6 \pm 3.0	28.1 \pm 0.0	42.4 \pm 0.9	73.4 \pm 0.7	86.5 \pm 0.7	91.2 \pm 0.0	93.1 \pm 0.4	93.6\pm0.2	94.1 \pm 0.2	94.3 \pm 0.0
CAL	12.9 \pm 2.0	15.8 \pm 4.1	19.2 \pm 4.5	63.0 \pm 1.4	72.2 \pm 0.2	78.1 \pm 0.9	82.6 \pm 0.5	85.0 \pm 0.2	87.6 \pm 0.7	89.6 \pm 0.4	93.0 \pm 0.2	94.3 \pm 0.0
DeepFool	11.6 \pm 0.7	14.6 \pm 1.3	15.6 \pm 4.1	47.3 \pm 6.8	71.7 \pm 1.1	84.2 \pm 0.4	90.0\pm0.2	91.6\pm0.1	92.4 \pm 0.2	93.2 \pm 0.2	94.1 \pm 0.1	94.3 \pm 0.0
Craig	13.3 \pm 1.4	14.2 \pm 1.4	13.6 \pm 0.0	46.6 \pm 0.0	67.3 \pm 3.1	82.4 \pm 0.6	88.8 \pm 0.3	91.4 \pm 0.0	92.7 \pm 0.2	93.4 \pm 0.1	94.2\pm0.1	94.3 \pm 0.0
GradMatch	13.4 \pm 2.0	13.0 \pm 2.3	13.0 \pm 0.0	44.6 \pm 3.7	53.9 \pm 1.4	77.9 \pm 0.4	87.2 \pm 0.3	90.2 \pm 0.6	92.6\pm0.0	93.4 \pm 0.0	94.2\pm0.1	94.3 \pm 0.0
Glister	15.7\pm0.0	13.9 \pm 3.0	18.9 \pm 5.0	44.0 \pm 4.0	53.5 \pm 0.9	78.2 \pm 2.2	86.4 \pm 0.1	89.7 \pm 0.0	92.5 \pm 0.2	93.3 \pm 0.2	94.2\pm0.1	94.3 \pm 0.0
Facility Location	12.6 \pm 1.3	16.8 \pm 2.5	15.3 \pm 2.5	48.0 \pm 6.9	73.4 \pm 0.7	85.4 \pm 0.3	89.5 \pm 0.3	90.6 \pm 0.3	92.5 \pm 0.2	93.2 \pm 0.1	94.1 \pm 0.1	94.3 \pm 0.0
SubZeroCore (ours)	12.8 \pm 0.6	18.0\pm0.0	17.7 \pm 3.2	65.7\pm1.7	78.1\pm0.4	86.9\pm0.2	88.8 \pm 0.3	90.7 \pm 0.1	91.9 \pm 0.1	92.2 \pm 0.0	93.7 \pm 0.1	94.3 \pm 0.0

Table 5: Coreset selection performances on CIFAR-10 with five randomly initialized ResNet-50 models. The best results are marked in bold.

Fraction ($1 - \alpha$)	0.1%	0.5%	1%	5%	10%	20%	30%	40%	50%	60%	90%	100%
Herding	16.2 \pm 2.4	23.0 \pm 2.4	29.5 \pm 2.8	46.3 \pm 2.8	58.5 \pm 5.2	73.1 \pm 2.1	80.0 \pm 0.9	84.1 \pm 0.5	86.4 \pm 0.9	89.6 \pm 0.9	94.6 \pm 0.3	95.4 \pm 0.3
k-Center Greedy	15.4 \pm 1.8	18.8 \pm 3.1	25.0 \pm 4.6	53.1 \pm 1.9	68.8 \pm 2.1	86.6 \pm 0.4	90.2 \pm 0.6	91.7 \pm 0.2	93.4 \pm 0.3	94.2 \pm 0.3	95.3 \pm 0.3	95.4 \pm 0.3
Forgetting	17.0 \pm 2.2	26.9 \pm 2.7	34.0 \pm 1.0	49.5 \pm 2.9	67.5 \pm 2.6	86.2 \pm 0.7	89.9 \pm 0.4	92.0 \pm 0.3	92.8 \pm 0.2	93.6 \pm 0.1	95.2 \pm 0.1	95.4 \pm 0.3
GraNd	15.1 \pm 1.7	17.2 \pm 1.4	19.7 \pm 1.2	23.6 \pm 1.6	34.9 \pm 2.4	70.3 \pm 5.0	85.5 \pm 1.4	92.0 \pm 0.3	94.2\pm0.4	94.9\pm0.4	95.4\pm0.2	95.4 \pm 0.3
CAL	19.9 \pm 1.3	27.5 \pm 0.6	35.9 \pm 1.2	56.4 \pm 1.4	66.2 \pm 1.1	77.6 \pm 0.8	83.0 \pm 0.4	85.5 \pm 0.5	88.2 \pm 0.5	90.5 \pm 0.6	94.2 \pm 0.2	95.4 \pm 0.3
DeepFool	14.4 \pm 2.0	19.8 \pm 1.4	26.4 \pm 1.1	42.7 \pm 2.9	65.7 \pm 2.8	86.3 \pm 0.9	91.1\pm0.5	92.9\pm0.3	93.9 \pm 0.2	94.5 \pm 0.2	95.3 \pm 0.2	95.4 \pm 0.3
Craig	17.0 \pm 1.1	21.5 \pm 1.4	28.1 \pm 2.6	42.0 \pm 1.5	55.1 \pm 2.7	80.8 \pm 2.8	89.9 \pm 0.7	92.5 \pm 0.7	93.5 \pm 0.2	94.7 \pm 0.1	95.4\pm0.2	95.4 \pm 0.3
GradMatch	14.3 \pm 2.8	21.7 \pm 0.9	28.2 \pm 0.9	37.4 \pm 2.6	50.5 \pm 3.5	74.0 \pm 2.3	87.6 \pm 1.1	92.3 \pm 0.4	93.8 \pm 0.3	94.7 \pm 0.5	95.2 \pm 0.2	95.4 \pm 0.3
Glister	14.9 \pm 0.9	20.4 \pm 1.5	24.2 \pm 3.3	37.0 \pm 1.9	50.1 \pm 3.0	79.6 \pm 2.5	88.6 \pm 0.8	92.0 \pm 0.3	93.5 \pm 0.2	94.5 \pm 0.3	95.2 \pm 0.2	95.4 \pm 0.3
Facility Location	16.6 \pm 1.4	20.1 \pm 4.0	32.9 \pm 2.0	55.9 \pm 2.4	71.1 \pm 3.6	86.7 \pm 1.0	90.8 \pm 0.4	92.7 \pm 0.2	93.7 \pm 0.5	94.4 \pm 0.3	95.1 \pm 0.3	95.4 \pm 0.3
SubZeroCore (ours)	20.1\pm0.5	27.8\pm0.2	36.5\pm0.7	57.6\pm3.3	74.6\pm0.9	86.8\pm0.7	90.0 \pm 0.2	91.4 \pm 0.3	92.8 \pm 0.3	93.3 \pm 0.3	95.3 \pm 0.1	95.4 \pm 0.3

Table 6: Coreset selection performances on CIFAR-10 with five randomly initialized InceptionNetV3 models. The best results are marked in bold.

Fraction (1 - α)	0.1%	0.5%	1%	5%	10%	20%	30%	40%	50%	60%	90%	100%
Herding	14.6 \pm 0.7	21.8 \pm 1.7	28.5 \pm 1.4	42.9 \pm 4.0	61.1 \pm 2.2	74.0 \pm 1.3	80.5 \pm 1.0	84.7 \pm 0.4	87.7 \pm 0.9	90.3 \pm 0.8	94.8 \pm 0.2	95.6 \pm 0.1
k-Center Greedy	15.1 \pm 2.0	22.1 \pm 3.0	26.6 \pm 1.4	51.2 \pm 2.3	72.9 \pm 1.7	85.8 \pm 0.4	89.8 \pm 0.4	92.2 \pm 0.3	93.6 \pm 0.3	94.4 \pm 0.4	95.4 \pm 0.2	95.6 \pm 0.1
Forgetting	18.5 \pm 0.6	28.5 \pm 1.0	32.2 \pm 0.9	50.9 \pm 1.5	69.3 \pm 1.3	85.4\pm0.9	90.4\pm0.4	92.4 \pm 0.1	93.4 \pm 0.2	94.3 \pm 0.3	95.4 \pm 0.2	95.6 \pm 0.1
GrANd	14.8 \pm 2.3	17.4 \pm 1.2	20.1 \pm 0.8	27.1 \pm 1.1	38.1 \pm 1.4	70.0 \pm 2.0	86.8 \pm 0.6	92.9\pm0.4	94.4\pm0.3	95.0\pm0.3	95.5 \pm 0.1	95.6 \pm 0.1
CAL	17.9 \pm 1.2	31.6 \pm 1.5	36.3 \pm 1.1	60.2 \pm 2.0	70.6 \pm 0.6	78.7 \pm 0.7	83.1 \pm 0.5	86.3 \pm 0.8	88.9 \pm 0.4	90.3 \pm 0.3	94.3 \pm 0.1	95.6 \pm 0.1
DeepFool	14.5 \pm 1.6	22.3 \pm 1.1	26.8 \pm 1.6	47.7 \pm 3.0	70.2 \pm 2.1	83.6 \pm 1.2	90.2 \pm 0.4	92.8 \pm 0.2	94.0 \pm 0.2	94.6 \pm 0.3	95.6\pm0.2	95.6 \pm 0.1
Craig	16.5 \pm 2.5	24.7 \pm 1.3	27.8 \pm 2.0	44.5 \pm 1.8	58.8 \pm 2.5	79.5 \pm 1.4	88.0 \pm 1.1	92.3 \pm 0.2	94.0 \pm 0.2	95.0\pm0.2	95.6\pm0.1	95.6 \pm 0.1
GradMatch	16.5 \pm 1.2	24.2 \pm 0.8	29.1 \pm 1.0	40.1 \pm 2.7	53.1 \pm 2.2	76.9 \pm 2.6	87.1 \pm 0.3	91.8 \pm 0.7	94.2 \pm 0.5	94.9 \pm 0.3	95.4 \pm 0.2	95.6 \pm 0.1
Glister	14.8 \pm 1.5	22.9 \pm 1.8	29.3 \pm 1.8	41.3 \pm 1.8	52.4 \pm 3.1	77.5 \pm 1.7	87.8 \pm 0.7	91.8 \pm 0.4	94.0 \pm 0.1	94.9 \pm 0.1	95.6\pm0.1	95.6 \pm 0.1
Facility Location	18.7\pm2.7	26.4 \pm 2.5	34.4 \pm 1.8	59.7 \pm 2.5	73.1 \pm 2.1	85.2 \pm 0.9	89.8 \pm 0.1	92.8 \pm 0.2	93.9 \pm 0.2	94.8 \pm 0.2	95.5 \pm 0.2	95.6 \pm 0.1
SubZeroCore (ours)	18.7\pm1.6	30.7\pm0.8	36.7\pm1.5	63.3\pm0.4	76.2\pm1.2	85.4\pm0.4	89.4 \pm 0.5	91.7 \pm 0.2	92.7 \pm 0.1	93.7 \pm 0.1	95.3 \pm 0.1	95.6 \pm 0.1

Table 7: Coreset selection performances on CIFAR-10 with five randomly initialized WRN-16-8 models. The best results are marked in bold.

Fraction (1 - α)	0.1%	0.5%	1%	5%	10%	20%	30%	40%	50%	60%	90%	100%
Herding	23.8 \pm 1.4	31.3 \pm 3.5	39.6 \pm 2.8	60.2 \pm 1.2	66.9 \pm 2.3	77.3 \pm 1.0	81.9 \pm 0.7	86.4 \pm 1.3	89.0 \pm 0.6	92.3 \pm 1.0	95.2 \pm 0.1	96.0 \pm 0.1
k-Center Greedy	19.2 \pm 0.6	27.7 \pm 0.6	34.6 \pm 0.2	67.9 \pm 0.8	81.6 \pm 0.5	89.4 \pm 0.2	92.1 \pm 0.3	93.6 \pm 0.2	94.3 \pm 0.1	94.9 \pm 0.1	95.9 \pm 0.1	96.0 \pm 0.1
Forgetting	21.5 \pm 1.0	30.1 \pm 0.9	36.3 \pm 0.6	58.5 \pm 1.0	74.9 \pm 0.8	88.8 \pm 0.5	93.3\pm0.1	94.5\pm0.1	95.0 \pm 0.1	95.4 \pm 0.1	95.9 \pm 0.1	96.0 \pm 0.1
GrANd	15.0 \pm 1.8	19.5 \pm 0.7	21.4 \pm 0.3	37.8 \pm 1.0	58.7 \pm 1.0	81.8 \pm 0.7	92.1 \pm 0.1	94.3 \pm 0.2	95.3\pm0.1	95.7\pm0.2	96.0\pm0.2	96.0 \pm 0.1
CAL	22.2 \pm 2.4	37.1 \pm 2.5	45.5 \pm 1.4	66.2 \pm 0.6	74.2 \pm 0.9	82.7 \pm 0.5	86.3 \pm 0.8	89.2 \pm 0.6	91.0 \pm 0.3	92.4 \pm 0.2	95.3 \pm 0.1	96.0 \pm 0.1
DeepFool	18.9 \pm 1.9	29.2 \pm 1.0	35.0 \pm 1.8	57.4 \pm 3.2	74.0 \pm 1.8	87.5 \pm 0.4	92.0 \pm 0.3	93.5 \pm 0.2	94.6 \pm 0.1	95.2 \pm 0.1	96.0\pm0.1	96.0 \pm 0.1
Craig	21.9 \pm 1.5	30.0 \pm 0.8	38.1 \pm 1.4	60.1 \pm 1.4	69.2 \pm 0.8	86.5 \pm 0.4	91.4 \pm 0.2	93.8 \pm 0.1	94.8 \pm 0.1	95.4 \pm 0.1	95.9 \pm 0.1	96.0 \pm 0.1
GradMatch	20.1 \pm 1.8	27.8 \pm 1.2	31.4 \pm 2.1	54.4 \pm 2.6	70.5 \pm 2.0	84.6 \pm 0.7	90.7 \pm 0.5	93.3 \pm 0.3	94.7 \pm 0.4	95.3 \pm 0.1	96.0\pm0.1	96.0 \pm 0.1
Glister	20.1 \pm 1.2	28.0 \pm 1.4	31.6 \pm 0.8	49.3 \pm 3.3	67.9 \pm 1.7	83.6 \pm 0.8	90.5 \pm 0.9	93.6 \pm 0.1	94.6 \pm 0.1	95.2 \pm 0.2	96.0\pm0.2	96.0 \pm 0.1
Facility Location	25.8 \pm 1.8	37.4 \pm 0.3	46.8 \pm 1.0	75.1 \pm 0.6	82.1 \pm 0.5	89.0 \pm 0.1	92.4 \pm 0.2	93.7 \pm 0.1	94.7 \pm 0.1	95.1 \pm 0.1	95.9 \pm 0.1	96.0 \pm 0.1
SubZeroCore (ours)	26.6\pm0.6	38.1\pm0.2	47.9\pm0.5	75.6\pm0.4	83.1\pm0.3	89.5\pm0.2	91.8 \pm 0.1	93.2 \pm 0.1	93.9 \pm 0.1	94.5 \pm 0.1	95.9 \pm 0.1	96.0 \pm 0.1

J SubZeroCore is submodular

We referred to *Berczi et al.* and omitted the proof in the main paper. For completeness, the proof can be done like the following.

Corollary 2. *The SubZeroCore function $f_{\text{SubZeroCore}}$ is submodular.*

Proof. Let $A \subseteq B \subseteq \mathcal{T}$ and pick any $k \in \mathcal{T} \setminus B$. For each $i \in \mathcal{T}$, define

$$\Delta_i(k \mid A) = \max(s_k \cdot \text{sim}(\mathbf{x}_i, \mathbf{x}_k), \max_{j \in A} s_j \cdot \text{sim}(\mathbf{x}_i, \mathbf{x}_j)) - \max_{j \in A} s_j \cdot \text{sim}(\mathbf{x}_i, \mathbf{x}_j).$$

Then the total marginal gain is

$$f(A \cup \{k\}) - f(A) = \sum_{i \in \mathcal{T}} \Delta_i(k \mid A), \quad f(B \cup \{k\}) - f(B) = \sum_{i \in \mathcal{T}} \Delta_i(k \mid B).$$

Since $\max_{j \in A} s_j \cdot \text{sim}(\mathbf{x}_i, \mathbf{x}_j) \leq \max_{j \in B} s_j \cdot \text{sim}(\mathbf{x}_i, \mathbf{x}_j)$, it follows for each i that $\Delta_i(k \mid A) \geq \Delta_i(k \mid B)$. Summing over i gives

$$f(A \cup \{k\}) - f(A) \geq f(B \cup \{k\}) - f(B),$$

which is exactly the diminishing-returns condition for submodularity.